XI International Conference on Computational Methods for Coupled Problems in Science and Engineering
COUPLED PROBLEMS 2025
A. Larese, S. Perotto and G. Rozza (Eds)

STOCHASTIC MODELLING OF PROTEIN AGGREGATION AND CLEARANCE IN BRAIN REGIONS USING A MULTISCALE FRAMEWORK FOR SIMULATING ALZHEIMER'S DISEASE

Hina Shaheen* **and Roderick Melnik†**

*Department of Statistics, Faculty of Science,
University of Manitoba, Winnipeg, MB R3T 2N2, Canada
e-mail: hina.shaheen@umanitoba.ca, web page: https://neurostatslab.com/

†MS2Discovery Interdisciplinary Research Institute
Wilfrid Laurier University, Waterloo, ON N2L 3C5, Canada
e-mail: rmelnik@wlu.ca, web page: https://m3ai.wlu.ca/

Key words: Neurodegenerative Disorders, Alzheimer's Disease, Large-scale Brain Network Model, Data-driven Methods, Wiener Process, Stochastic modelling

Abstract. *Neurodegenerative diseases such as Alzheimer's are characterized by the abnormal accumulation and spread of misfolded protein aggregates across different brain regions. To capture the spatiotemporal dynamics and inherent variability of these processes, we develop a multiscale stochastic framework that models protein aggregation, fragmentation, and clearance using Smoluchowski-type equations extended to brain-wide simulations. The model incorporates size-dependent clearance rates and stochastic fluctuations to reflect biological uncertainty, and includes diffusion-driven transport between anatomically distinct brain regions. We simulate multiple aggregate species (c_1 to c_N) across seven representative brain areas and analyze ensemble outcomes to extract probability densities, toxic load evolution, and spatial progression patterns. Our results reveal region-specific differences in aggregation kinetics, with pronounced variability in higher-order aggregates and late-stage toxic burden. This work presents a flexible and biologically grounded modelling framework for studying protein dynamics in neurodegenerative progression, offering insights into the role of stochasticity in brain-wide aggregate distribution.*

1 INTRODUCTION

Neurodegenerative disorders such as Alzheimer's disease (AD) are marked by the gradual accumulation, misfolding, and spread of toxic protein aggregates such as amyloid-beta and tau, throughout the brain [1, 2]. These aggregates originate as monomeric proteins and, through a series of biophysical interactions, form complex oligomeric and fibrillar structures that interfere with neuronal function, leading to cognitive and functional decline [3, 16]. Understanding the mechanisms that govern the formation, fragmentation, clearance, and inter-regional propagation of these aggregates remains a fundamental challenge in neuroscience and mathematical biology [4, 5].

The brain is not a spatially uniform organ; it consists of interconnected regions, each with distinct anatomical structures, metabolic properties, and levels of vulnerability to neurodegenerative processes [1, 6]. In this study, we focus on seven major brain regions that are known to be either early targets or critical hubs in neurodegenerative pathways: the frontal, parietal, temporal, and occipital lobes, as well as the limbic system, basal ganglia, and brainstem. These regions are involved in essential cognitive, motor, emotional, and autonomic functions, and exhibit varying susceptibilities to protein misfolding and accumulation. For instance, the temporal lobe (especially the entorhinal cortex and hippocampus) is often the first to show signs of amyloid or tau pathology in AD. At the same time, the brainstem and basal ganglia are involved in motor-related neurodegeneration, such as Parkinson's disease [7].

To model the dynamics of protein aggregation across these heterogeneous regions, we develop a stochastic, multiscale framework grounded in aggregation-fragmentation theory. Our model extends classical Smoluchowski equations to incorporate several critical biological features: (i) binary aggregation of smaller species into larger aggregates, (ii) symmetric binary fragmentation of larger species into smaller ones, (iii) size-dependent clearance, capturing the reduced removal efficiency of larger aggregates, and (iv) diffusive transport between brain regions, enabling the spatial spread of aggregates [2]. Most importantly, we embed this system within a stochastic framework, using the Euler–Maruyama scheme to account for intrinsic biological noise and population-level variability [7].

In this study, we focus exclusively on Case II adopted from our previous study [2], which incorporates the essential biological mechanisms of aggregation, fragmentation, clearance and stochasticity. This case offers a comprehensive yet tractable representation of protein dynamics in the brain. In this framework, smaller protein species can combine to form larger aggregates through pairwise interactions, while larger aggregates can break apart into smaller units via symmetric binary fragmentation. To reflect the biological challenge of removing toxic species from the brain, we introduce size-dependent clearance rates that decrease in efficiency for larger aggregates. Aggregation is modelled through binary interactions between species to form larger aggregates, while fragmentation allows these larger species to break into smaller ones. Size-dependent clearance is included to reflect the reduced efficiency of biological clearance mechanisms for larger aggregates. Most critically, stochastic fluctuations are introduced to capture intrinsic biological variability and region-specific uncertainty in aggregate evolution. Case II thus provides the most realistic framework for simulating neurodegenerative progression without the added complexity of irreversible deposition or nucleation thresholds, as seen in other cases. Each brain region is modelled as a node in a connected network, allowing for both local intra-region dynamics and inter-region interactions via diffusion. By simulating the concentrations of protein species from monomers (c_1 to c_N) across these regions, we explore both the temporal evolution and spatial heterogeneity of toxic load in the brain. Through ensemble simulations, we extract key metrics, including region-specific toxic burden, probability distributions of aggregate sizes, and uncertainty in disease progression pathways.

This stochastic model provides a biologically realistic and computationally flexible framework for studying the emergence and spread of neurodegeneration in the human brain. It also offers potential for extending to patient-specific or data-driven applications using neuroimaging or biomarker data.

2 GENERAL THEORY AND STOCHASTIC MODELLING APPROACH

In this section, we extend the deterministic Smoluchowski framework by incorporating stochasticity to better capture the biological variability and uncertainty in protein aggregation, fragmentation, and astrocytic clearance [2]. Neurodegenerative disease progression is inherently noisy due to cell-level randomness, environmental fluctuations, and variability in brain structure and function across individuals [8]. A stochastic model provides a natural mechanism to represent these uncertainties [9, 15].

2.1 Stochastic Smoluchowski Model on Brain Networks

Let $c_{i,j}(t)$ denote the concentration of protein aggregates of size i at node j of the brain network at time t, where $i = 1, 2, \ldots, N$ and $j = 1, 2, \ldots, V$, with V denoting the number of brain regions (e.g., $V = 1015$ in a fine-resolution parcellation). We model the evolution of $c_{i,j}(t)$ as a stochastic differential equation (SDE) of the form:

$$\frac{dc_{i,j}}{dt} = -i^{-\eta} \sum_{k=1}^{V} L_{jk} c_{i,k} + F_{i,j}(c(t)) + \sigma_{i,j}(c(t)) dW_{i,j}(t), \tag{1}$$

where, L_{jk} is the graph Laplacian of the brain connectome, capturing anisotropic diffusion between regions, rest of the terms represents deterministic reaction terms including nucleation, aggregation, fragmentation, and clearance adopted from [2]. In addition, $\sigma_{i,j}(c(t))$ is a noise coefficient dependent on species size and possibly the region, $dW_{i,j}(t)$ is a Wiener process (standard Brownian motion), introducing stochastic fluctuations [8]. The deterministic term $F_{i,j}(c(t))$ in the SDE is defined analogously to the classical Smoluchowski model [2]:

$$F_{i,j}(c(t)) = -\left(\mu_{i,j} + \frac{\beta_{i,j}}{2}(i-1)\right) c_{i,j} + \alpha c_{1,j}(c_{i-1,j} - c_{i,j}) + \sum_{k=1}^{N-i-1} \beta_{i+k,j} c_{i+k,j}, \tag{2}$$

where, $\mu_{i,j}$ is the clearance rate for aggregates of size i at region j, and $i = 3, \ldots, N-1$ and $j = 1, \ldots, V$. These terms are preserved from the deterministic formulation and now contribute to the drift term of the stochastic system.

2.2 Biological Interpretation of Noise Model

The stochastic term $\sigma_{i,j}(c(t))dW_{i,j}(t)$ accounts for intrinsic fluctuations due to variability in astrocytic clearance efficacy across regions and over time. Moreover, randomness in aggregation rates from local concentration effects and environmental variability, and fluctuations in transport along axonal pathways. We consider a multiplicative noise model of the form:

$$\sigma_{i,j}(c) = \epsilon_i \cdot c_{i,j},$$

where $\epsilon_i \ll 1$ is a small parameter controlling the fluctuation intensity for species of size i.

Thus, the full stochastic model becomes:

$$dc_{i,j}(t) = \left[-i^{-\eta} \sum_{k=1}^{V} L_{jk} c_{i,k} + F_{i,j}(c(t))\right] dt + \epsilon_i c_{i,j}(t)\, dW_{i,j}(t). \tag{3}$$

However, due to the absence of closed-form solutions, we employ numerical simulation using a Monte Carlo ensemble approach. The SDE is discretized using the Euler–Maruyama scheme:

$$c_{i,j}^{n+1} = c_{i,j}^{n} + \Delta t \cdot F_{i,j}(c^n) - \Delta t \sum_k L_{jk} c_{i,k}^{n} + \epsilon_i c_{i,j}^{n} \cdot \Delta W_{i,j}^{n},$$

where $\Delta W_{i,j}^{n}$ are independent Gaussian random variables with zero mean and variance Δt. The simulation is repeated L times to generate an ensemble:

$$\left\{ c_{i,j}^{n,m} \right\}_{m=1}^{L},$$

from which we compute statistical summaries, such as the mean, variance, and probability distributions of aggregate concentrations across brain regions and time. Over the entire brain network, to better understand the development of toxic proteins, we compute the toxic mass as a function of time at each node:

$$M_j(t) = \sum_{i=2}^{N} c_{i,j}(t), \quad j = 1, \ldots, V,$$

we average the toxic mass of all regions considered in the present study, e.g. the usual four lobes: basal ganglia, temporal, parietal, frontal, occipital along with the limbic region, basal ganglia and brain stem. Also,

$$M^j = \frac{1}{x_j} \sum_{i \in X_j} M_i, \quad j = 1, \ldots, 7,$$

where X_j is defined as the set of all nodes in that region and x_j is the number of elements of X_j[2].

3 RESULTS

To investigate the spatial and temporal progression of protein aggregation in neurodegenerative disorders, we simulated the stochastic aggregation-fragmentation dynamics across seven anatomically distinct brain regions:frontal, parietal, temporal, occipital, limbic, basal ganglia, and brainstem. Using ensemble simulations of the stochastic Smoluchowski model with size-dependent clearance, symmetric binary fragmentation, and inter-regional diffusion, we captured both average behaviours and variability in aggregate concentrations over time.

We tracked the concentrations of monomers (c_1) through higher-order oligomers (c_N) in each region. The simulations reveal a progressive depletion of monomers and a corresponding increase in intermediate and large-sized aggregates, consistent with the pathological signature of protein misfolding diseases. The growth of higher-order species was most pronounced in the temporal and limbic regions, reflecting their known vulnerability in the early stages of AD. For instance, Figure 1 illustrates the temporal evolution of toxic protein aggregate mass across seven brain regions:frontal, parietal, temporal, occipital, limbic, basal ganglia, and brainstem. The y-axis represents the total concentration of high-order aggregates (typically c_n for $n \geq 6$), while the $x - axis$ shows time in simulation steps. Each colored curve corresponds to the mean aggregate mass in a region, and the shaded bands indicate the stochastic variability across 30

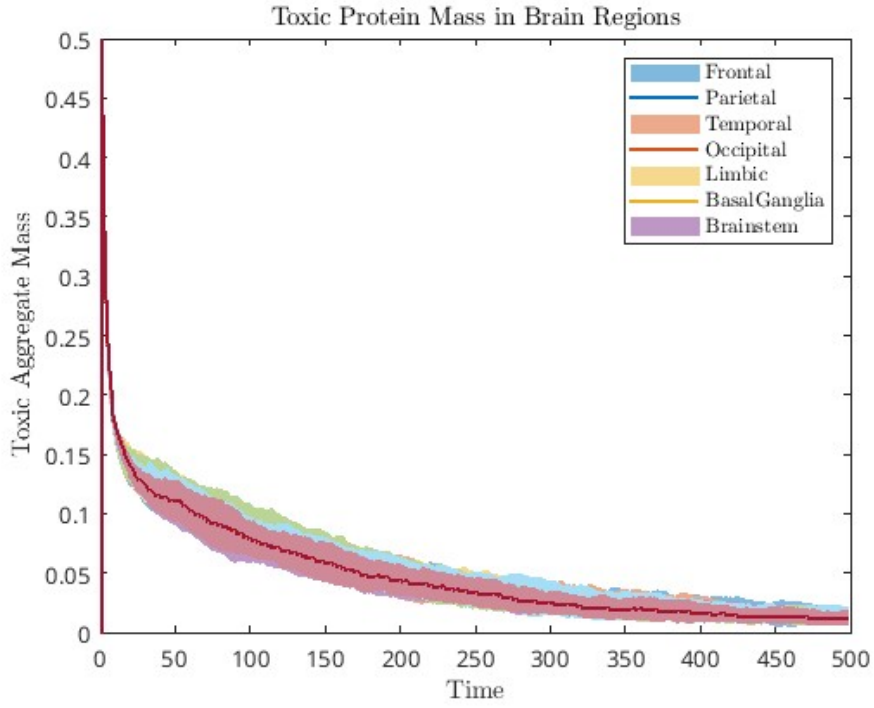

Figure 1: The temporal evolution of toxic protein aggregate mass across seven brain regions:frontal, parietal, temporal, occipital, limbic, basal ganglia, and brainstem

ensemble runs. The results reveal a general decline in toxic mass over time, suggesting that clearance and fragmentation processes dominate under the current parameter settings. Despite uniform network connectivity, spatial heterogeneity emerges: the brainstem and limbic regions retain higher toxic loads longer, whereas regions like the frontal and parietal clear aggregates more efficiently. The variability bands highlight biological noise and underscore the importance of stochastic modelling to capture regional uncertainty in disease progression. This figure demonstrates the model's ability to reflect both global trends and localized variability in neurodegenerative dynamics.

Figure 2 presents a heatmap visualization of the spatiotemporal evolution of toxic protein aggregates across seven major brain regions. The $x - axis$ represents simulation time, while the $y - axis$ enumerates the distinct brain regions. The color scale reflects the concentration of toxic protein aggregates (defined as species of size $n \geq 6$), averaged over all ensemble runs. Warmer colors (yellow and white) indicate higher concentrations, whereas darker shades (red to black) correspond to lower levels of toxic mass. This figure highlights the initial widespread seeding of toxic aggregates, followed by a gradual and region-specific clearance over time. Notably, the temporal and limbic regions exhibit slightly elevated concentrations during the early and middle phases of simulation, suggesting greater susceptibility or delayed clearance in these areas. In contrast, the frontal, parietal, and brainstem regions demonstrate a more rapid decline in toxic load. The spatiotemporal map captures both the heterogeneous spread and decay of aggregate burden across the brain, supporting the hypothesis that structural and regional variability, even in a symmetric network model, leads to distinct patterns of disease progression. This visualization complements the ensemble-averaged plots by providing a compact overview of regional dynamics across time.

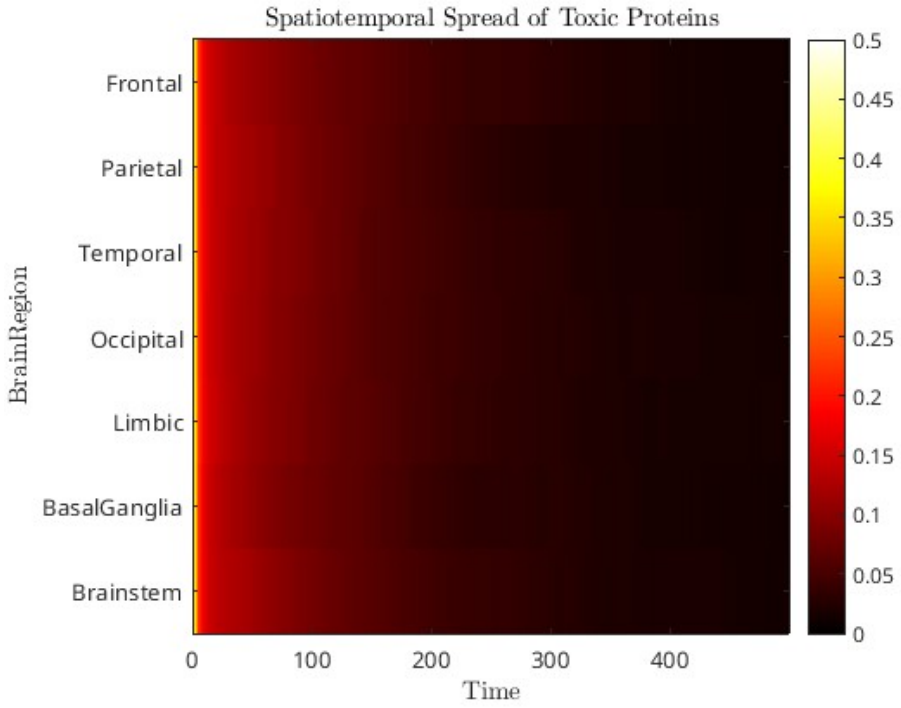

Figure 2: The visualization of the spatiotemporal evolution of toxic protein aggregates across seven major brain regions:frontal, parietal, temporal, occipital, limbic, basal ganglia, and brainstem

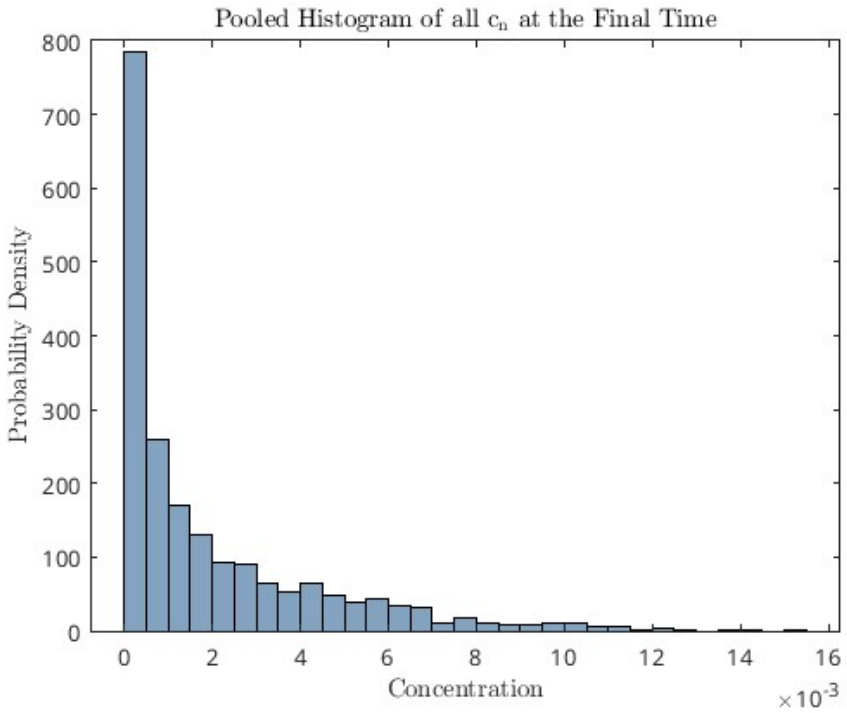

Figure 3: The probability density histogram of the protein aggregate concentrations, pooled across all brain regions

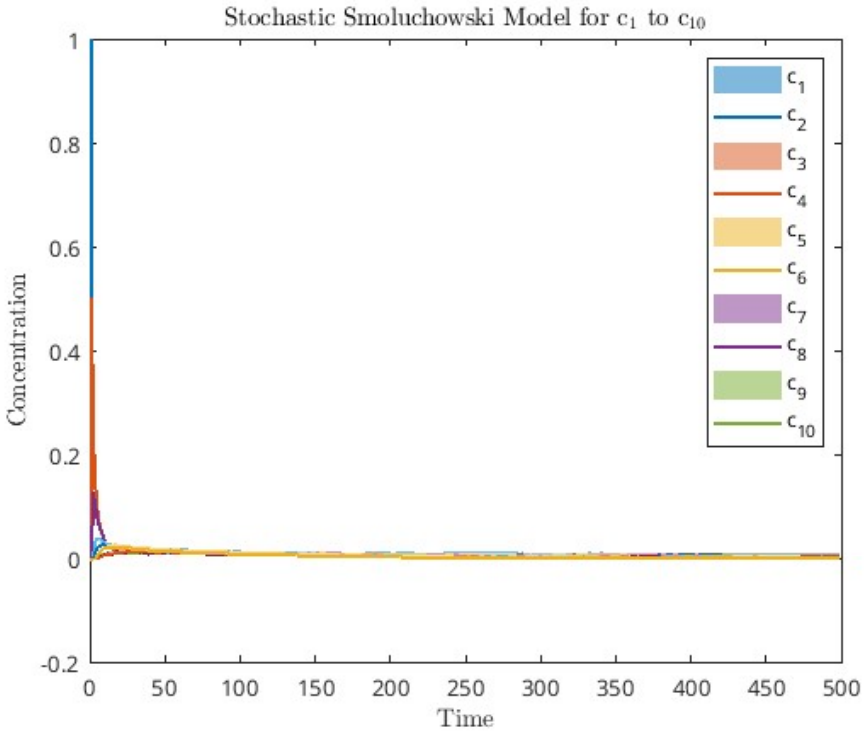

Figure 4: The time evolution of protein aggregate species c_1 through c_{10} under the stochastic Smoluchowski framework, pooled over all brain regions and ensemble runs

To quantify uncertainty, we analyzed the probability density functions (PDFs) of aggregate concentrations c_n across all ensemble runs at selected time points. Figure 3 presents a probability density histogram of the protein aggregate concentrations, pooled across all brain regions, all species sizes, and all ensemble runs at the final simulation time point. The $x - axis$ shows the concentration values, while the $y - axis$ displays the corresponding probability density. The histogram reflects the distribution of aggregate species at the end of disease progression under the stochastic simulation framework. The distribution is heavily skewed toward lower concentrations, with the majority of species registering values near zero. This indicates that most aggregates are either cleared or present in negligible amounts by the end of the simulation. A long tail extending toward higher concentrations represents rare but persistent aggregates, which may correspond to resilient toxic species or regions with delayed clearance. This result highlights the heterogeneity in local concentrations, even after a global decline in total toxic load, and provides a statistical summary of the stochastic variability and clearance efficacy across the brain. The concentration-dependent asymmetry also supports the need for probabilistic modelling in neurodegenerative disease simulations.

Figure 4 illustrates the time evolution of protein aggregate species c_1 through c_{10} under the stochastic Smoluchowski framework, pooled over all brain regions and ensemble runs. The $x - axis$ represents time, and the $y - axis$ shows the concentration of each aggregate species. Each curve corresponds to a specific aggregate size, from monomers (c_1) to decamers (c_{10}), and their stochastic average trajectories are visualized using color-coded lines. At the start of the simulation, monomers (c_1) are highly abundant, reflecting the uniform initial seeding. As aggregation proceeds, monomers are rapidly consumed to form higher-order species such as

dimers (c_2), trimers (c_3), and so on. However, due to the combined effects of fragmentation, clearance (with size-dependent rates), and diffusion, all species—including the larger aggregates—exhibit sharp declines in concentration and eventually stabilize near zero. The rapid decay and near-zero equilibrium levels suggest that, under the modelled conditions, the system reaches a quasi-steady state dominated by clearance and fragmentation. The lack of persistent accumulation implies that the clearance mechanisms are effective, especially for larger aggregates that are removed more efficiently due to the size-dependent clearance rate $\mu_n \propto n$. This figure supports the conclusion that even though aggregation is initiated across all regions, the long-term presence of toxic species is transient in this simulation scenario. It also reinforces the importance of stochastic effects in shaping the temporal profile of each aggregate class.

4 DISCUSSION

This study presents a multiscale stochastic modelling framework for simulating the dynamics of protein aggregation in neurodegenerative disorders (NDDs) across anatomically distinct brain regions [1]. By extending the classical Smoluchowski equations to incorporate inter-regional diffusion, size-dependent clearance, and biologically motivated stochasticity, our approach provides a more realistic and spatially resolved perspective on the mechanisms underlying disease progression [2].

The results demonstrate distinct spatiotemporal patterns of aggregate accumulation, with the temporal and limbic regions exhibiting faster growth and higher concentrations of large aggregates [10]. These observations are consistent with clinical and postmortem findings in AD, where the hippocampus and entorhinal cortex are among the earliest regions to show pathology. The model captures regional heterogeneity in both aggregate load and variability, which deterministic frameworks often overlook [11]. One of the key strengths of the stochastic approach is its ability to represent uncertainty and variability that arise from biological noise, environmental fluctuations, and inter-individual differences [2]. The ensemble simulations revealed that even with identical initial conditions and parameters, the disease burden can vary significantly across runs, particularly in later stages and for larger aggregate species [12, 13]. This result aligns with the heterogeneous clinical presentation of NDDs, where disease onset and progression vary markedly between individuals.

Moreover, the use of the brain network topology modelled via the Laplacian of the connectome enables the exploration of how structural connectivity influences the spatial distribution of pathology [2, 5]. Diffusive coupling between regions facilitates the spread of aggregates, mimicking the transneuronal propagation observed in prion-like mechanisms. Our framework thus supports the hypothesis that both local aggregation kinetics and long-range structural connections shape the landscape of neurodegeneration [6, 14].

Importantly, the model also allows for the examination of therapeutic strategies. By modulating parameters such as clearance rates, diffusion strengths, or noise amplitudes, one can simulate the potential impact of treatments aimed at enhancing protein degradation, disrupting aggregation, or stabilizing oligomeric intermediates. Future extensions could include patient-specific connectomes or biomarker-informed parameterization to enable personalized simulation of disease trajectories. Overall, the proposed stochastic model offers a powerful platform for understanding the dynamics of protein aggregation in the brain, emphasizing the importance of variability, spatial context, and network-driven propagation. These insights contribute to a growing body of evidence that supports the need for probabilistic, region-aware approaches to

model and potentially mitigate neurodegenerative diseases.

5 CONCLUSIONS

In this work, we have developed a stochastic, multiscale modelling framework to simulate protein aggregation and clearance dynamics across multiple brain regions, with a specific focus on the spatial progression of neurodegenerative disorders. By extending classical aggregation-fragmentation models with region-specific stochasticity, size-dependent clearance, and inter-regional diffusion, our approach captures both the deterministic trends and the inherent biological variability observed in disease propagation.

The results demonstrate that distinct brain regions exhibit varied susceptibilities to aggregate accumulation, with the temporal and limbic regions emerging as early and prominent sites of toxic load. Through ensemble simulations, we have shown that stochastic effects significantly influence disease trajectories, leading to a wide range of outcomes even under identical initial conditions. This variability aligns well with clinical observations of inter-individual heterogeneity in neurodegeneration. Our findings underscore the importance of incorporating uncertainty and spatial structure into models of protein misfolding diseases. The framework presented here provides a flexible platform for exploring disease mechanisms, evaluating region-specific vulnerability, and simulating potential therapeutic interventions. Future extensions may include integration with patient-specific imaging data or application to other neurodegenerative conditions such as Parkinson's or Huntington's disease. Finally, this work contributes to the growing body of systems neuroscience approaches that aim to bridge molecular pathology with large-scale brain dynamics using data-driven, probabilistic modelling techniques.

REFERENCES

[1] Shaheen, H. and Melnik, R. Brain Network Dynamics and Multiscale Modeling of Neurodegenerative Disorders: A Review. *IEEE Access.* (2025) **13**: 33074-33100.

[2] Shaheen, H., Pal, S. and Melnik, R. Astrocytic clearance and fragmentation of toxic proteins in Alzheimer's disease on large-scale brain networks. *Physica D: Nonlinear Phenomena*. (2023) **454**: 133839.

[3] Candelise, N., Scaricamazza, S., Salvatori, I., Ferri, A., Valle, C., Manganelli, V., Garofalo, T., Sorice, M. and Misasi, R. Protein aggregation landscape in neurodegenerative diseases: Clinical relevance and future applications. *International journal of molecular sciences*. (2021) **22**(11): 6016.

[4] Limorenko, G. and Lashuel, H.A. Revisiting the grammar of Tau aggregation and pathology formation: how new insights from brain pathology are shaping how we study and target Tauopathies. *Chemical Society Reviews*. (2022) **51**(2): 513-565.

[5] Shaheen, H., Melnik, R., Singh, S. and Alzheimer's Disease Neuroimaging Initiative. Data-driven stochastic model for quantifying the interplay between amyloid-beta and calcium levels in Alzheimer's disease. *Statistical Analysis and Data Mining: The ASA Data Science Journal*. (2024) **17**(2): e11679.

[6] MacIver, A. and Shaheen, H. Modelling Alzheimer's Protein Dynamics: A Data-Driven Integration of Stochastic Methods, Machine Learning and Connectome Insights. *arXiv e-prints*. (2024): 2411.

[7] Shaheen, H. and Melnik, R. Bayesian approaches for revealing complex neural network dynamics in Parkinson's disease. *Journal of Computational Science*. (2025) **85**: 102525.

[8] Guantes, R., Díaz-Colunga, J. and Iborra, F.J. Mitochondria and the non-genetic origins of cell-to-cell variability: More is different. *Bioessays*. (2016) **38**(1): 64-76.

[9] Shaheen, H., Melnik, R. and Alzheimer's Disease Neuroimaging Initiative. Bayesian inference and role of astrocytes in amyloid-beta dynamics with modelling of Alzheimer's disease using clinical data. *arXiv preprint*. (2023) **2306**: 12520.

[10] Lim, J. and Yue, Z. Neuronal aggregates: formation, clearance, and spreading. *Developmental cell.* (2015) **32**(4): 491-501.

[11] Lam, B., Masellis, M., Freedman, M., Stuss, D.T. and Black, S.E. Clinical, imaging, and pathological heterogeneity of the Alzheimer's disease syndrome. *Alzheimer's research & therapy*. (2015) **5**(1):1.

[12] Meentemeyer, R.K., Cunniffe, N.J., Cook, A.R., Filipe, J.A., Hunter, R.D., Rizzo, D.M. and Gilligan, C.A. Epidemiological modeling of invasion in heterogeneous landscapes: spread of sudden oak death in California (1990–2030). *Ecosphere*. (2011) **2**(2): 1-24.

[13] Eisele, Y.S., Monteiro, C., Fearns, C., Encalada, S.E., Wiseman, R.L., Powers, E.T. and Kelly, J.W. Targeting protein aggregation for the treatment of degenerative diseases. *Nature reviews Drug discovery*. (2015) **14**(11): 759-780.

[14] Kreiser, R.P., Wright, A.K., Block, N.R., Hollows, J.E., Nguyen, L.T., LeForte, K., Mannini, B., Vendruscolo, M. and Limbocker, R. Therapeutic strategies to reduce the toxicity of misfolded protein oligomers. *International journal of molecular sciences*. (2020) **21**(22): 8651.

[15] Hadjichrysanthou, C., Ower, A.K., de Wolf, F., Anderson, R.M. and Alzheimer's Disease Neuroimaging Initiative. The development of a stochastic mathematical model of Alzheimer's disease to help improve the design of clinical trials of potential treatments. *PloS one*. (2018) **13**(1): e0190615.

[16] Frisoni, G.B., Altomare, D., Thal, D.R., Ribaldi, F., van der Kant, R., Ossenkoppele, R., Blennow, K., Cummings, J., van Duijn, C., Nilsson, P.M. and Dietrich, P.Y. The probabilistic model of Alzheimer disease: the amyloid hypothesis revised. *Nature Reviews Neuroscience*. (2022) **23**(1): 53-66.